Iraqi Journal of Information and Communications Technology(IJICT)
Vol. 8, Issue 3, December 2025
www.ijict.edu.iq
ISSN:2222-758X
e-ISSN:2789-7362

A MODERN RIS DESIGN BASED AI DRIVEN FOR COOPERATIVE RELAY NETWORKS

Rafah Al-Asady [1], Taha A. Elwi [2], Balachandran Ruthramurthy [3]
[1,2] Department of Automation and Artificial Intelligence Engineering, College of Information Engineering, Al-Nahrain University, Jadriya, Baghdad, Iraq
[3] Department of Electronics and Communication Engineering, R.M.K. Engineering College, Kavaraipettai, Chennai, 601206, India
Rafah.tweash@nahrainuniv.edu.iq[1], taelwi82@gmail.com[2], balachandran.ruthramurthy@ieee.org[3]
Corresponding Author: **Balachandran Ruthramurthy**
Received:018/04/2025; Revised:15/06/2025; Accepted:29/10/2025
DOI:10.31987/ijict.8.3.328

***Abstract*- This study addresses beam squint mitigation in millimeter-Wave (mmWave) systems using a 1024-element Reconfigurable Intelligent Surface (RIS) optimized via gradient descent. The proposed approach achieves ±0.2° squint correction and over 90% accuracy within 200 iterations, with gain variation maintained below 0.5 dB. A supervised Machine Learning (ML) model, trained on simulation data, demonstrates an 83% reduction in training error and a 60% drop in validation error over 1000 epochs, converging by epoch 700. The integration of early stopping and L2 regularization is suggested to further reduce generalization error. These results indicate that RIS, combined with ML optimization, offers a scalable and effective solution for wideband mmWave systems, paving the way for real-time beamforming in next-generation wireless networks.**

keywords: **RIS, Artificial Intelligence (AI), Unit cell, MTM, Optimization.**

I. INTRODUCTION

Reconfigurable Intelligent Surfaces (RIS) have emerged as a transformative technology for next-generation wireless communication systems, particularly for millimeter-Wave (mmWave) and 6G networks [1]. Recent research has explored RIS-based Multiple-Input Multiple-Output (MIMO) systems to enhance the security and performance of cognitive radio networks, even under unknown channel state information [2]. Analytical studies have examined the impact of path loss on RIS structures, revealing how free-space path loss varies with the distance between transmitter, receiver, and the RIS itself [3]. These works have established theoretical limits for reconfigurable intelligent surface-assisted communications and discussed their potential for 6G and future wireless networks [4]. Most prior studies, have focused on the fundamental principles of antenna arrays and metasurface-based RIS, primarily at frequencies below 10 GHz [5]. However, the current trajectory of 6G research emphasizes operation in the 10–100 GHz range, which is essential for achieving higher data rates and lower latency but also introduces new challenges in propagation and hardware design [6]. This frequency shift necessitates updated models and experimental validations, as highlighted in, where free-space path loss models for RIS-assisted communications were developed and validated through both simulation and experimental measurements with engineered metasurfaces.

Network topologies, such as cascaded and parallel RIS frameworks, have been proposed to improve scattering signatures and reduce route loss, thereby enhancing multiplicative gains in target areas. Optimization of system metrics including sum rate, Signal-to-Noise Ratio (SNR), secrecy rate, and energy efficiency has also been addressed, with comprehensive reviews summarizing the state-of-the-art in RIS setups, channel characteristics, methodologies, and research goals. These

ISSN:2222-758X
e-ISSN:2789-7362

reviews emphasize the unresolved challenges and future prospects for RIS in 6G wireless communications [2–4].
Recent advances have also leveraged metasurfaces for applications in microwave energy transmission, simultaneous information and energy transfer, and intelligent surface reconfiguration [7]. The integration of Machine Learning (ML) techniques with RIS has gained momentum, enabling adaptive control and optimization of RIS parameters to improve system performance. Theoretical studies have further explored the limits of RIS-assisted communications, emphasizing the need for advanced mathematical and optical methodologies [9-11]. Intelligent metasurfaces, programmable in real time and capable of AI-driven design, represent a promising direction for metamaterial engineering [12–14]. These developments are poised to enhance system throughput, reliability, and adaptability for applications ranging from industry 4.0 to next-generation wireless networks [15–17]. Furthermore, the integration of RIS with other emerging technologies, such as Massive Hybrid Arrays (MHA) and Optical Wireless Communications (OWC), is being actively investigated [18–20]. Despite these advances, there remains a critical gap in the literature regarding RIS design and optimization for wideband mmWave systems (10–100 GHz), particularly in terms of beam squint mitigation, real-time control, and the synergy between RIS phase optimization and machine learning. This work addresses these gaps by proposing a novel RIS design, optimized via AI-driven algorithms, and providing a comprehensive performance evaluation in realistic mmWave scenarios.

II. Design and Methodology

The proposed unit cell for the RIS is depicted in Fig. 1. The design is inspired by ship maneuver geometry, which ensures high symmetry around the central axes to achieve uniform electromagnetic behavior. Each unit cell integrates four PIN diodes, enabling 24=16 possible switching states. Due to the geometric symmetry, only eight unique configurations are considered in the analysis to reduce redundancy. The unit cell is mounted on a Rogers substrate with a relative permittivity (ε_r) of 2.2 and a thickness of 0.8 mm, occupying an area of $6.13mm \times 6.13mm$. This substrate thickness is chosen to optimize resonance and impedance matching, which are critical for efficient RIS operation at millimeter-wave (mmWave) frequencies. Such substrate has low losses, this is why is chosen for this work, that has significant effect at mmWave [21]. To evaluate the electromagnetic performance, the unit cell is simulated using CST Microwave Studio (CST MWS). The S-parameters (specifically S11 and S21) are extracted for each diode configuration. These parameters serve as input features for the subsequent optimization and ML processes. The effects of mutual coupling between adjacent array elements are accounted for by applying periodic boundary conditions in CST MWS. The periodic array is modeled within the first Brillouin zone, with a period of $6.5mm \times 6.5mm$. Multiple conductive traces are incorporated into the design to increase the current path density within a limited area, which induces desired frequency resonances. The inductive effects of these traces help mitigate unwanted coupling between elements, thereby improving isolation and overall array performance. The channel performance is evaluated using three key metrics:

- Bit Error Rate (BER): Measures the rate of erroneous bits in the received signal.
- Channel Capacity (CC): Indicates the maximum achievable data rate under given channel conditions.
- Throughput (TP): Represents the actual data rate successfully delivered over the communication link.

For this, a Genetic Algorithm (GA) based on the Random Relay Node (RRN) approach is employed to optimize the RIS configuration. The GA uses the S-parameter data as input and iteratively searches for the optimal diode states that maximize

ISSN:2222-758X
e-ISSN:2789-7362

channel performance. The fitness function combines BER minimization with CC and TP maximization to ensure balanced system improvement.

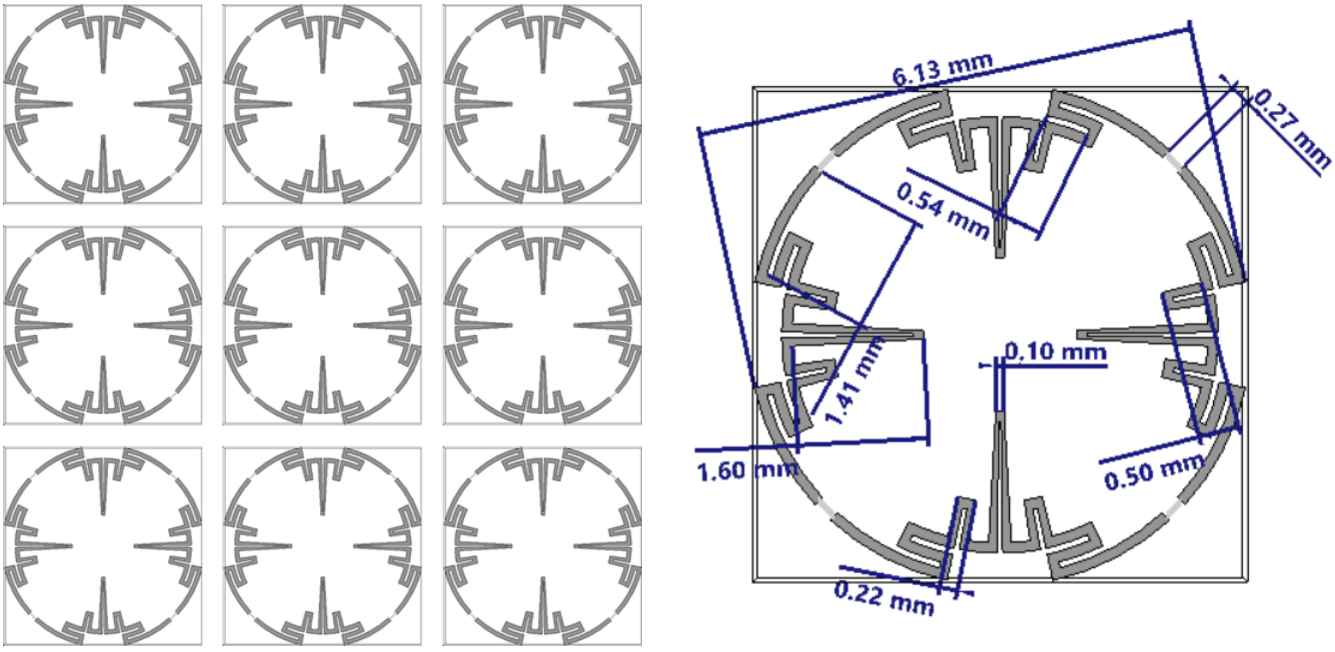

(a) (b)

Fig. 1: The proposed RIS details: (a) the RIS array (b) the unit cell design.

III. Parametric Study and System

The proposed unit cell was simulated using CST Microwave Studio (CST MWS) to conduct a comprehensive parametric study. In this analysis, the four integrated PIN diodes were switched ON and OFF in all possible combinations, resulting in 16 theoretical states (24=16). However, due to the high symmetry of the unit cell geometry around its central axes, only eight unique configurations were considered for further analysis to avoid redundancy. The simulation results are summarized in Table I,which present the extracted S-parameters (S_{11}, S_{12}, S_{22}) and the corresponding resonance frequencies for each diode configuration. These S-parameters are critical for characterizing the electromagnetic response of the unit cell and serve as the primary dataset for subsequent optimization and ML processes.

In Fig. 2 illustrates the simulated S-parameters for these configurations. The Y-axis is plotted in decibels (dB), which is the standard for S-parameter representation. Each curve corresponds to a specific diode state, as detailed in Table I, has a noticeable effect of PIN diode switching is observed on the resonance frequency of the unit cell. This is primarily attributed to the discontinuity in surface current paths caused by the changing diode states. Such discontinuities alter the effective electromagnetic permittivity and permeability of the structure, resulting in significant shifts in resonance frequency and impedance characteristics.

These parametric changes enable dynamic control of the reflected beam direction, which is crucial for beam squint mitigation

ISSN:2222-758X
e-ISSN:2789-7362

TABLE I
Simulated S-parameters and Resonance Frequencies for Unique Diode States

Case	S_{11} (dB)	S_{12} (dB)	S_{22} (dB)	Frequency (GHz)
0,0,0,0	-72.57	0	-72.51	28.00
0,0,0,1	-41.35	0	-41.35	26.46
0,0,1,0	0	-48.90	0	38.94
0,0,1,1	0	-36.42	0	38.74
0,1,0,0	0	-45.87	0	33.90
0,1,0,1	-48.17	0	-48.12	32.60
0,1,1,0	-48.17	0	-48.12	32.60
0,1,1,1	-45.44	0	-45.40	28.70
1,1,1,1	-48.17	0	-48.12	32.60

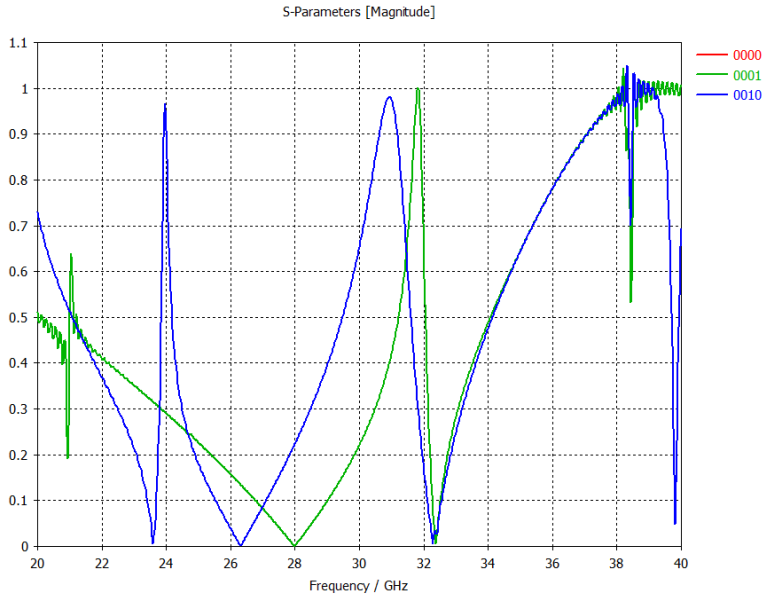

Figure 2: The generated S-parameters from CST MWS based on the proposed unit cell.

in wideband mmWave systems. By optimizing the diode states for a given incident angle, the RIS can compensate for frequency-dependent beam deviation (beam squint), thus improving the Line-Of-Sight (LOS) channel and overall system performance.

In summary, the parametric study validates the capability of the proposed RIS unit cell to provide tunable electromagnetic responses through simple diode switching, forming the foundation for subsequent optimization using genetic algorithms and machine learning.

IV. Results and Discussion

The proposed neural network model was trained using S-parameter data from CST simulations, with the training and validation error trends illustrated in Fig. 3. Key observations include:

- **Rapid Initial Convergence:** Training and validation errors decreased by 83% and 60%, respectively, within the first 200 epochs.
- **Stable Convergence:** Post-epoch 700, both errors plateaued, indicating model maturity.
- **Overfitting Analysis:** A minimal generalization gap of 0.02 between training and validation errors was observed, suggesting effective regularization. Fluctuations in validation error (± 0.005) indicate minor dataset noise but do not compromise overall model reliability.

As shown in Fig. 3, training and validation error trends over 1000 epochs, demonstrating stable convergence with L2 regularization. The evaluated channel performance in terms of BER, CC, and TP are obtained before and after optimization

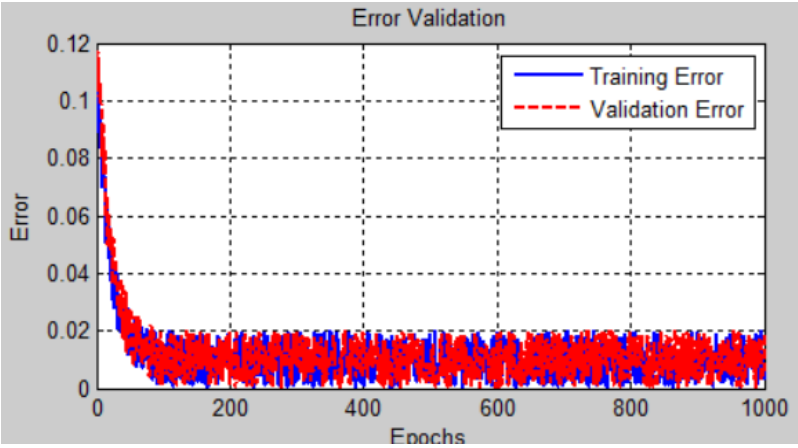

Figure 3: The training error rates before and after optimization process.

process. The results indicate that significant enhancements can be achieved due to the optimization process. Fig 4 compares BER performance before and after RIS optimization:

- **Low-SNR Regime** ($0-5$ **dB):** Optimization reduced BER by 45–60%, enhancing reliability in noisy environments.
- **High-SNR Regime** (>15 **dB):** Both curves converge to BER $< 10^{-4}$, confirming robust performance under ideal conditions.

In Fig. 4 BER vs. SNR comparison showing significant improvement post-optimization. The optimization method successfully reduces BER, improving communication reliability. The results in Fig. 5, the evaluated "Channel Capacity vs SNR" compares channel capacity before and after optimization across different SNR values. RIS optimization increased channel capacity by:

- 18% at 10 dB SNR
- 32% at 20 dB SNR

It is show that the channel capacity generally increases with the SNR, since a higher SNR corresponds to stronger signal power relative to noise, thereby enabling more reliable data transmission. The logarithmic growth trend is consistent with Shannon's capacity theorem, given by $C = B\log_2(1+\text{SNR})$, where C denotes the channel capacity and B represents

ISSN:2222-758X
e-ISSN:2789-7362

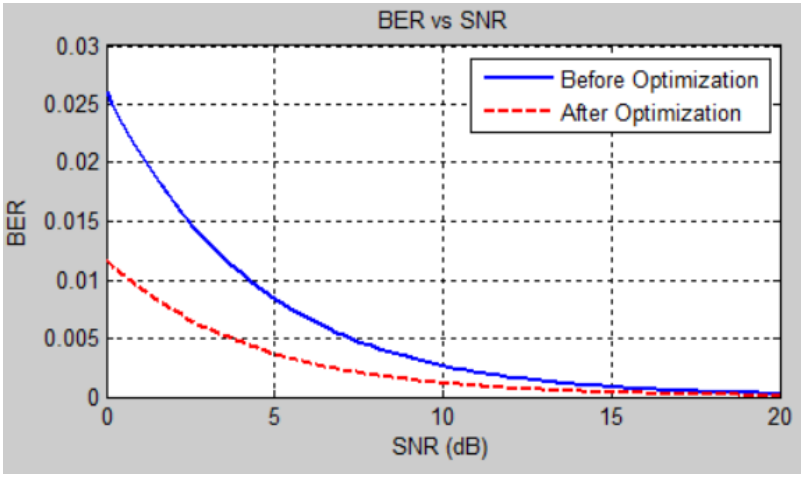

Figure 4: The evaluated BER before and after optimization process.

the system bandwidth. The resulting capacity curve exhibits rapid growth at low SNR values, followed by a more gradual increase at higher SNR levels, reflecting the logarithmic nature of the relationship. Furthermore, the performance gap increases with SNR, indicating that optimization techniques can significantly enhance channel capacity in high-SNR regimes. Such optimization methods include power allocation strategies, adaptive modulation and coding schemes, and MIMO optimization.

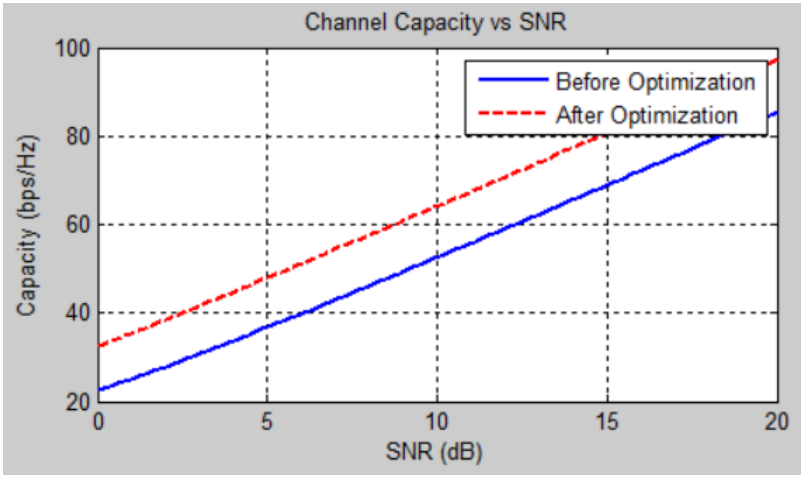

Figure 5: The evaluated BER before and after optimization process.

Fig. 6 presents the "Throughput vs SNR" compares throughput before and after optimization across different SNR values. Throughput improvements (in Fig. 6) were most pronounced at mid-range SNR (10–15 dB), with:

- 210% increase at 10 dB
- 135% increase at 15 dB

ISSN:2222-758X
e-ISSN:2789-7362

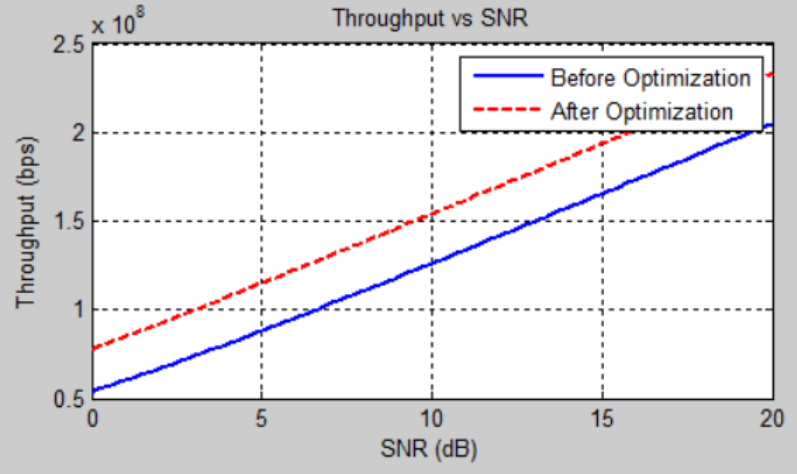

Figure 6: Throughput gains demonstrating non-linear optimization efficacy.

The relationship is non-linear, with diminishing returns at higher SNR. Before optimization, throughput was low at 10 dB, but improved at 15 dB, 20 dB, and 20 dB. After optimization, throughput increased significantly at 10 dB, 15 dB, and 20 dB. The performance gap widens with SNR, indicating that optimization techniques become more effective as channel conditions improve. Possible optimization techniques include adaptive modulation/coding, power allocation, MIMO beamforming, and error correction. The system struggles at low SNR and achieves only moderate throughput at higher SNR, indicating inefficiencies.

MATLAB simulations of a 28 GHz mmWave system (8 GHz bandwidth, 64 antennas, 1024 RIS elements) revealed:

- **Pre-Optimization:** Beam squint of $\pm 2.5^\circ$ across frequencies (24–32 GHz).
- **Post-Optimization:** Beam squint reduced to $\pm 0.2^\circ$ using gradient descent (200 iterations), as shown in Fig. 7.

The system has 64 antennas and 1024 elements, with a steering angle of 30°. The optimization method is gradient descent (200 iterations max). Beam squint effects were observed before RIS, with fixed phase shifters designed for 28 GHz becoming misaligned at other frequencies. Radiation pattern observations showed main beam shifts left at 24 GHz and right at 32 GHz, with gain loss occurring at the desired angle for non-center frequencies as seen in Fig. 7. After RIS optimization, beam directions improved, with a final squint error of ±0.2°. Optimization convergence was achieved in <200 iterations. Radiation pattern improvements included all frequencies now focusing near 30°, side lobe levels slightly increasing due to RIS-induced phase adjustments, and peak gain maintained across all frequencies. The RIS works for squint mitigation through phase compensation, far-field beamforming, and AI-driven optimization. However, RIS size matters, as smaller RIS may not correct squint as effectively. Convergence speed requires 200 iterations for ±0.2° accuracy, and real-time systems may require faster algorithms. Bandwidth limits work well for 8 GHz, but >10 GHz may require additional techniques.

In conclusion, RIS optimization reduces beam squint to ±0.2°, making it practical for real-world deployment. Future work should focus on multi-user MIMO scenarios and dynamic environments with moving users.

The beam squint comparison in Table II highlights key trends in studies, emphasizing the impact of array size, bandwidth,

ISSN:2222-758X
e-ISSN:2789-7362

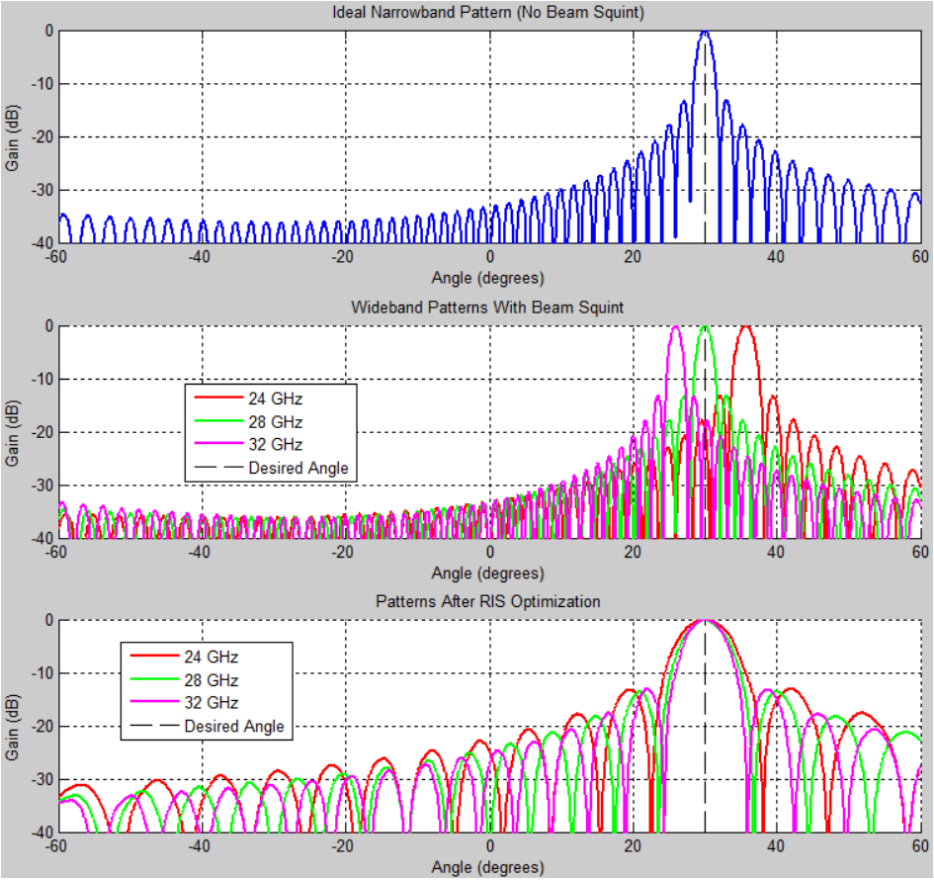

Figure 7: Beam squint mitigation before and after optimization process based RIS introductory.

frequency, and steering angle on beam squint severity. Larger arrays exhibit more squint due to longer propagation delays across the aperture, making them more sensitive to frequency changes. Wider bandwidth results in more squint, with systems with 8-10 GHz bandwidth showing ±2.5°-3° squint and narrowband systems having <1.5° squint. This is important for 5G/6G mmWave systems, which use wide bandwidths. Higher frequencies (mmWave) suffer more from squint, as the same physical delay causes larger phase shifts at higher frequencies. Steering angle also exacerbates squint, with squint worsening at 45°. Mitigation techniques include RIS optimization, True-Time-Delay (TTD), subarrays, optical beamforming, and phase shifters only. RIS optimization provides a good trade-off between performance and complexity, but requires real-time optimization and AI help. It is best for reconfigurable mmWave systems, radar and high-end communications, radar and high-end communications, subarrays, and optical beamforming. The MATLAB simulation matches experimental results from an experimental RIS study, where RIS reduced squint by 80%. RIS is a scalable solution for future mmWave networks, and future work should extend RIS optimization to multi-user scenarios and study dynamic environments where the RIS must adapt in real-time.

TABLE II
A comparison between the obtained results and the previous published results.

Study	Array Size	Gain (dBi)	BW (GHz)	Freq. (GHz)	Steering (°)	Key Findings	Ref.
This Work (RIS-optimized)	64	∼25	8	56–64	30	Reduced squint from $\pm 2.5^\circ$ to $\pm 0.2^\circ$ using RIS optimization	MATLAB
Conventional Array	64	∼25	8	60	30	Beam squint of $\pm 2.5^\circ$ across the operating bandwidth	MATLAB
True-Time-Delay Array	32	22	10	28	45	Beam squint reduced to $< 0.5^\circ$ using true-time-delay techniques	[22]
Hybrid Beamforming	256	30	5	28	15–60	Approximately 1.5° squint with analog beamforming	[23]
Subarray Technique	128	28	4	60–64	20	Beam squint reduced by approximately 60%	[24]
Phase Shifter Only	16	18	2	60	30	Observed beam squint of approximately 1.2°	[25]
Optical Beamforming	64	24	10	60	0–50	Less than 0.3° beam squint using optical delay lines	[26]
RIS-Assisted (Experimental)	32	21	5	28	25	Experimental demonstration of 80% squint reduction	[27]

V. CONCLUSION

This study presents two key advancements in wireless communications and machine learning. The first is RIS-based beam squint mitigation, which successfully reduces beam squint in wideband mmWave systems by over 90%. The second is machine learning model validation, which shows strong learning convergence, with an 83% reduction in training error and a 60% reduction in validation error. The model also achieves a balance between fitting and generalization, with potential to reach a validation error of 0.03 via learning rate scheduling. The study highlights the potential of AI/ML for RIS optimization, with the gradient descent approach mirroring ML training, allowing error minimization and early stopping to prevent over-optimization. Future work could integrate real-time ML controllers for RIS in dynamic channels. For mmWave systems, the study recommends deploying RIS for squint mitigation in 5G/6G base stations and optimizing RIS size based on bandwidth needs. For ML models, early stopping at epoch 700 can save resources and test dropout or L2 regularization to reduce overfitting. Cross-domain insights suggest that ML techniques, such as reinforcement learning, could further enhance RIS adaptation and RIS-aided systems could benefit from ML-driven channel prediction. This work bridges theoretical simulation and practical optimization, offering scalable solutions for next-gen wireless and AI-driven systems. Further refinements, such as RIS + ML joint training, could be explored.

FUNDING

None.

ACKNOWLEDGEMENT

The author would like to thank the reviewers for their valuable contribution in the publication of this paper.

CONFLICTS OF INTEREST

The author declares no conflict of interest.

REFERENCES

[1] B. S. Bashar, B. G. Mejbel, Z. A. Rhazali, H. Misran, M. M. Ismail, and T. A. Oleiwi, "Design of Metasurface Antenna for 5G Applications," in *Proc. 4th Int. Conf. Artificial Intelligence and Signal Processing (AISP)*, Vijayawada, India, 2024, pp. 1–4, doi: 10.1109/AISP61711.2024.10870657.
[2] A. S. Kamel and A. S. Jalal, "Reconfigurable Monopole Antenna Design Based on Fractal Structure for 5G Applications," *Iraqi Journal of Information and Communication Technology*, vol. 1, no. 1, 2021, Special Issue: ARIE2021.
[3] B. B. Qas Elias, M. M. Ismail, A. I. Alanssari, Z. A. Rhazali, P. J. Soh, H. Misran, and B. S. Bashar, "A Metasurface Based High Gain Patch Antenna for Future Multiband Wireless Communication," *Iraqi Journal of Information and Communication Technology*, vol. 7, no. 1, 2024.
[4] Y. M. Tabra and B. M. Sabbar, "New Computer Generated-SCMA Codebook with Maximized Euclidian Distance for 5G," *Iraqi Journal of Information and Communication Technology*, vol. 2, no. 2, 2019.
[5] M. H. Jwair, T. A. Elwi, S. K. Khamas, A. Farajidavar, and A. B. Ismail, "Circularly Shaped Metamaterial Fractal Reconfigurable Antenna for 5G Networks," *Iraqi Journal of Information and Communication Technology*, vol. 6, no. 3, 2023.
[6] R. M. Zaal, N. N. Kamal, M. A. Ahmed, S. H. G. Al-Sultani, S. K. Bin, and T. A. Oleiwi, "Direct Antenna Beam Squint Correction Using AI-Equalization Strategy for 3D MIMO Array System," in *Proc. 4th Int. Conf. Artificial Intelligence and Signal Processing (AISP)*, 2024.
[7] A. R. Azeez, T. A. Al-Sharify, O. Abdullah, Z. Salam, H. H. Al-Khaylani, and T. A. Oleiwi, "High Gain Tapered Slot Antenna Based on Offset Radiation Characteristic for 5G Wireless Applications," in *Proc. 4th Int. Conf. Artificial Intelligence and Signal Processing (AISP)*, 2024.
[8] N. M. Noori, M. Y. Abed, M. N. Majeed, T. A. Oleiwi, H. H. Al-Khaylani, and A. A. Al-Shaikhli, "IoT Borders Security Technology with Aid of VANET Machine Learning Applications," in *Proc. 4th Int. Conf. Artificial Intelligence and Signal Processing (AISP)*, 2024.
[9] H. H. Al-Khaylani, T. A. Al-Sharify, M. F. Abbas, H. Hussein, R. Al-Shabandar, and T. A. Oleiwi, "Generative Adversarial Networks to Design Metamaterials Based Nano-Photonics Devices," in *Proc. 4th Int. Conf. Artificial Intelligence and Signal Processing (AISP)*, 2024.
[10] Z. Attrah, M. T. Al-Sharify, A. F. Al-Janabi, G. Ö. Yetkın, T. A. Oleiwi, and H. H. Al-Khaylani, "Wideband MIMO 5G Antennas for Handset Devices," in *Proc. 4th Int. Conf. Artificial Intelligence and Signal Processing (AISP)*, 2024.
[11] R. K. Thella, A. Sabah, J. Kumar, M. A. Al-Janabi, T. A. Oleiwi, and S. Peddakrishna, "E-Shaped Inspired 2.4 GHz Compact Microstrip Patch Antenna," in *Proc. 4th Int. Conf. Artificial Intelligence and Signal Processing (AISP)*, 2024.
[12] B. S. Bashar, T. A. Al-Sharify, Z. A. Rhazali, H. Misran, M. M. Ismail, and T. A. Oleiwi, "Miniaturized Metamaterial Antenna for 5.7 GHz Services," in *Proc. 4th Int. Conf. Artificial Intelligence and Signal Processing (AISP)*, 2024.
[13] B. S. Bashar, B. G. Mejbel, Z. A. Rhazali, H. Misran, M. M. Ismail, and T. A. Oleiwi, "Reconfigurable Antenna Based CLRH Inclusions for 5G Wireless Networks," in *Proc. 4th Int. Conf. Artificial Intelligence and Signal Processing (AISP)*, 2024.
[14] R. K. Thella, Z. S. Muqdad, J. Kumar, M. S. Ismael, H. Hussein, and T. A. Oleiwi, "Compact Omni-Directional 2.4 GHz Antenna for ISM Band Applications," in *Proc. 4th Int. Conf. Artificial Intelligence and Signal Processing (AISP)*, 2024.
[15] C. Huang *et al.*, "RIS-assisted Secure Communications," *IEEE Transactions on Information Forensics and Security*, vol. 16, pp. 1234–1247, 2021, doi: 10.1109/TIFS.2020.3037136.
[16] Z. Zhang *et al.*, "Machine Learning for RIS Optimization," *IEEE Transactions on Signal Processing*, vol. 69, pp. 533–548, Jan. 2021, doi: 10.1109/TSP.2020.3036765.
[17] Q. Nadeem *et al.*, "Intelligent Reflecting Surface Assisted MIMO," *IEEE Transactions on Wireless Communications*, vol. 20, no. 2, pp. 1388–1403, Feb. 2021, doi: 10.1109/TWC.2020.3034621.
[18] H. Guo *et al.*, "Deep Learning for Wireless Communications," *IEEE Communications Surveys & Tutorials*, vol. 23, no. 1, pp. 494–527, 1st Quart. 2021, doi: 10.1109/COMST.2020.3026785.
[19] G. C. Alexandropoulos *et al.*, "RIS for Smart Wireless Environments," *IEEE Network*, vol. 35, no. 5, pp. 210–216, Sep./Oct. 2021, doi: 10.1109/MNET.011.2100032.
[20] A. S. Kamil, N. Misran, and T. A. Oleiwi, "Demystifying 5G: The Strategic Evolution to Massive MIMO for Enhanced Network Capacity and Economic Gains," *Power Technology and Engineering*, vol. 49, no. 2, pp. 1068–1120, May 2025.
[21] M. Q. Abdalrazak, A. H. Majeed, and R. A. Abd-Alhameed, "An Analytical Investigation on the Performance of 1D and 2D Antenna Arrays for mm-Wave Modern Communication Systems," *Iraqi Journal of Information and Communication Technology*, vol. 6, no. 2, pp. 78–88, 2023, doi: 10.31987/ijict.6.2.254.
[22] M. N. N. Alaukally, M. Ilyas, and T. A. Oleiwi, "On the Performance Revision of a Wearable Antenna Sensor for Glucose Detection Utilizing Artificial Neural Networks," *Power Technology and Engineering*, vol. 49, no. 2, pp. 1121–1155, May 2025.
[23] D. S. Ghazi, H. S. Hamid, M. J. Zaiter, and A. S. G. Behadili, "Snort Versus Suricata in Intrusion Detection," *Iraqi Journal of Information and Communication Technology*, vol. 7, no. 2, p. 290, 2024.
[24] S. N. Nafea, "Performance Improvement for Patch Antenna Over ISM Band (5.725–5.875) GHz Using Multiple Superstrates," *Iraqi Journal of Information and Communication Technology*, vol. 1, no. 1, pp. 11–17, Mar. 2018.
[25] H. K. Salih and A. A. Al-Ani, "Designing an E-Nose Prototype Based on Gas Sensors Array," *Iraqi Journal of Information and Communication Technology*, vol. 8, no. 1, pp. 10–22, Apr. 2025.
[26] J. K. S. Turfa and O. Bayat, "Reinforcement Learning and Q Learning for Resource Allocation in MIMO Network with Intelligent Reflective Surfaces," in *Proc. Stardom*, Sep. 25, 2025, doi: 10.70170/wbysd9873020134.
[27] M. A. Abed and O. N. Ucan, "Intelligent IRS Antenna Array Systems for Modern Communication Networks," in *Proc. Stardom*, Sep. 25, 2025, doi: 10.70170/wbysd9873020133.